The effects of complex chemistry on triple flames

By T. Echekki[1] and J. H. Chen[1]

The structure, ignition, and stabilization mechanisms for a methanol (CH_3OH)-air triple flame are studied using Direct Numerical Simulations (DNS). The methanol (CH_3OH)-air triple flame is found to burn with an asymmetric shape due to the different chemical and transport processes characterizing the mixture. The excess fuel, methanol (CH_3OH), on the rich premixed flame branch is replaced by more stable fuels CO and H_2, which burn at the diffusion flame. On the lean premixed flame side, a higher concentration of O_2 leaks through to the diffusion flame. The general structure of the triple point features the contribution of both differential diffusion of radicals and heat. A mixture fraction-temperature phase plane description of the triple flame structure is proposed to highlight some interesting features in partially premixed combustion. The effects of differential diffusion at the triple point add to the contribution of hydrodynamic effects in the stabilization of the triple flame. Differential diffusion effects are measured using two methods: a direct computation using diffusion velocities and an indirect computation based on the difference between the normalized mixture fractions of C and H. The mixture fraction approach does not clearly identify the effects of differential diffusion, in particular at the curved triple point, because of ambiguities in the contribution of carbon and hydrogen atoms' carrying species.

1. Introduction

Triple flames arise in a number of practical configurations where the reacting mixture is partially premixed. The flame has three branches reflecting the extent of premixedness of the fuel and oxidizer. On the fuel side, a rich premixed flame forms, while on the oxidizer side, a lean premixed flame forms. Behind the two branches, a diffusion flame forms where 'excess' fuel and oxidizer burn. The premixed flame branches provide both a source of reactants (excess from the primary premixed flames) for the diffusion flame and a mechanism for its stabilization and ignition at the triple point (the location where the three branches meet).

During the last two decades a number of studies of triple flames have been carried out to understand the mechanisms of stabilization and their structure using simplified models of chemistry and transport (Hartley & Dold, 1991; Kioni *et al.*, 1993; Lakkaraju, 1996; Ruetsch *et al.*, 1995; Domingo & Vervisch, 1996; and Wichman, 1995). Recently, computations by Terhoeven & Peters (1996) have shown

1 Sandia National Laboratories

the significance of complex chemistry and realistic transport to the structure and stabilization of triple methane-air flames.

In the context of complex chemistry and transport effects, a number of questions pertaining to the flame structure, ignition at the triple point and propagation remain unanswered. The structure of the premixed flame on the rich and lean branches is expected to be asymmetrical because of the inherent asymmetry in the flammability limits, reacting mixture composition, and burning rates of the flame. In the diffusion branch, the primary fuel may not be the original fuel that burns on the premixed side. In the computations of Terhoeven & Peters (1996), only a small fraction of the primary fuel, methane, survives near the triple point. Instead, more stable molecules such as CO and H_2 provide the needed fuel to burn in the diffusion flame.

Moreover, the diffusion flame is anchored to the premixed branches at the triple point by both preheating and diffusion of radicals including H, O, and OH. These radicals diffuse at rates which are significantly different from diffusion rates of heat and result in differential diffusion effects at the triple point. The coupling of curvature and differential diffusion effects at the triple point may also display itself in enhanced burning rates and, thereby, enhanced propagation of the triple point. The same differential diffusion effects along with chemistry determine the structure and location of the diffusion branch of the triple flame.

The object of this study is to determine the structure and mechanisms of ignition and stabilization of triple methanol (CH_3OH)-air flames in a laminar free shear layer configuration using detailed chemistry and a realistic transport model. The choice of methanol as a fuel presents some advantages with regard to the complexity of the chemical system and the numerical treatment. The full range of flammability may be adequately described using C_1 chemistry. It displays some of the interesting features in its structure which are common among hydrocarbons (e.g. the two-layer structure corresponding to fuel- and radical consumption, and H_2 and CO oxidation). In the following sections, the governing equations and numerical configuration are described. A discussion of the triple flame structure and the contribution of chemistry and transport to its ignition and stabilization is presented.

2. Governing equations and numerical configuration

The triple flame in a laminar mixing layer between methanol (CH_3OH) fuel and air as oxidizer is computed using DNS with a C_1 mechanism for chemistry (Warnatz *et al.*, 1996). The numerical scheme is based on the solution of the Navier-Stokes, species, and energy equations for a compressible gas mixture with temperature dependent properties. The equations are solved using an eighth-order explicit finite difference scheme (Kennedy & Carpenter, 1994) for approximating spatial derivatives and a fourth-order low storage Runge-Kutta scheme for time advancement (Kennedy & Carpenter, 1996). A modified version of the Navier-Stokes Characteristic Boundary Conditions (NSCBC) procedure originally developed by Poinsot & Lele (1992) is used to account for variable specific heats (Card *et al.*, 1994). The

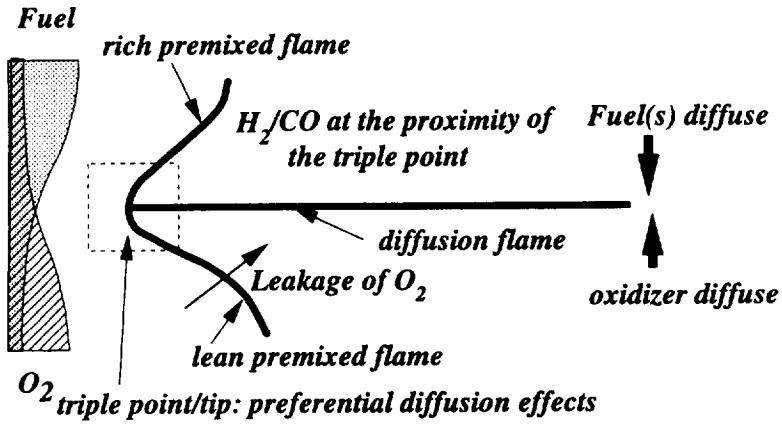

FIGURE 1. Numerical configuration.

boundary conditions are non-reflecting in all directions. The species mass diffusion is modeled with a Lewis number formulation and a prescription of the Lewis numbers for the different species (Smooke & Giovangigli, 1991). The values of the Lewis numbers for the species is given in Table 1. The Prandtl number, $Pr = \mu \overline{C}_p/\lambda$, is set to a constant of 0.708.

For the C_1 methanol (CH_3OH) mechanism, conservation equations for fifteen reacting species are considered (see Table 1), and the mass fraction of N_2 is obtained through the relationship $\sum_{\alpha=1}^{N} Y_\alpha = 1$, where $N = 16$. The computational configuration is shown in Fig. 1. The initial mixture is preheated to 800 K. The field is initialized with stoichiometric one-dimensional flame profiles which are modified spatially over a buffer domain of thickness L to reflect the desired inlet composition. The inlet conditions are maintained constant during the computations. The inlet velocity is fixed at the stoichiometric flame speed, S_L; no attempt to stabilize the flame is made. The methanol, oxygen, and its corresponding proportion of nitrogen (in air) in the buffer domain are based on self-similar solution profiles of the mixture fraction, ξ. They are prescribed as follows:

$$\xi(x,y,t=0) = (1-\xi_{st}) \cdot \left\{1 - \exp\left[-\left(\frac{x-L}{\Delta}\right)^2\right]\right\} \Big/ \left\{1 - \exp\left[-\left(\frac{L}{\Delta}\right)^2\right]\right\} \cdot \operatorname{erf}\left(\frac{y}{\delta}\right) + \xi_{st}. \tag{1}$$

Here, ξ is the mixture fraction expressed as follows:

$$\xi \equiv \frac{Z^* - Z_O^*}{Z_F^* - Z_O^*},$$

where the subscripts F and O denote the fuel and oxidizer streams, respectively. Z^* is expressed in terms of the elemental mixture fraction (three elements make up the reacting species: C, H, and O), Z_i as follows (Warnatz *et al.*, 1996):

$$Z^* = \sum_{i=1}^{\text{elem.}} \beta_i \, Z_i. \tag{2}$$

The element mass fraction, Z_i, is defined as $Z_i = \sum_{\alpha=1}^{N} \mu_{i\alpha} Y_\alpha, \quad \alpha = 1, \ldots, N$, where $\mu_{i\alpha}$ is the mass proportion of the element i in the species α (e.g. for hydrogen atom in methane, it is 1/4). In terms of the species mass fraction, Z^* may be written as $Z^* = \sum_{\alpha=1}^{N} \mu_\alpha^* \, Y_\alpha$, where $\mu_\alpha^* = \sum_{i=1}^{\text{elem.}} \beta_i \, \mu_{i\alpha}$.

species	Le
H_2	0.30
O_2	1.11
O	0.70
OH	0.73
H_2O	0.83
H	0.18
HO_2	1.10
H_2O_2	1.12
CO	1.10
CO_2	1.39
CH_2O	1.28
CHO	1.27
CH_2OH	1.30
CH_3OH	1.30
CH_3O	1.30

TABLE 1. Lewis Numbers of Reacting Species.

In Eq. 1, ξ_{st} denotes the stoichiometric mixture fraction; δ is the characteristic thickness of the mixing region in the y direction; Δ is the buffer region characteristic thickness. In the spatial and temporal variations, the rate of variations of mixture fraction profiles in x are specified as Gaussian functions with characteristic thicknesses, Δ. For hydrocarbon fuels, Bilger *et al.* (1990) propose $2/W_C$, $1/(2W_H)$ and $1/W_O$ as coefficients β_i (Eq. 2) for the carbon (C), hydrogen (H), and oxygen (O) elements. Here, W_C, W_H and W_O are the atomic weights of C, H, and O. The proposed coefficients have been used in turbulent methanol diffusion flames by Masri *et al.* (1992). The stoichiometric mixture fraction for the methanol-air mixture based on these coefficients is $\xi_{st} = 0.136$.

A single computation is carried out with a mixture fraction characteristic thickness of $\delta/\delta_F = 3.5$. The flame thermal thickness, δ_F, corresponds to the stoichiometric premixed methanol-air flame and is defined as follows:

$$\delta_F = \frac{T_b - T_u}{(dT/dx)_{max}},$$

where the subscripts u and b refer, respectively, to the unburnt and burnt gases. The buffer domain size, L/δ_F, and its characteristic thickness, Δ/δ_F, are 5.4 and 0.7, respectively. The computational domain is 501 by 351 grid points.

3. Numerical diagnostics

The DNS yields detailed information about the flow field and various scalars characterizing the structure of the triple flame. In this section, diagnostic approaches used to identify the pertinent features of the triple flame are described.

3.1 Reaction flow analysis

The primary objective of reaction flow analysis (Warnatz *et al.*, 1996) is to identify the primary reactions which contribute to the production or consumption of a particular species or to the rate of heat release.

3.2 Quantitative analysis of differential diffusion effects

Differential diffusion represents a non-negligible phenomenon in hydrogen and hydrocarbon flames in regions of strong curvature. It contributes to the enhancement of the burning intensity due to the strong chemical role played by hydrogen atoms and molecules in these flames and their fast rate of diffusion. To identify the strength of differential diffusion effects, in particular at the triple point in the flame, two approaches are considered. The first is based on the computation of the diffusion velocities of the various reactive species in the mixture which represent a direct measure of differential diffusion effects. From the formulation described earlier, the diffusion velocity of species, α, may be written as follows:

$$V_{\alpha j} = -D_{\alpha N}\frac{1}{Y_\alpha}\frac{\partial Y_\alpha}{\partial x_j}, \quad \alpha = 1, \cdots, N-1.$$

An alternate and indirect method of identifying strong differential diffusion effects is to compute the difference between elemental mass fractions (Bilger, 1981; Bilger & Dibble, 1982; Drake & Blint, 1988; Smith *et al.*, 1995). In the present work, the difference, $z_{C,H}$, between elemental mass fractions of C atom and H atoms is computed:

$$z_{C,H} = \xi_C - \xi_H,$$

where

$$\xi_C \equiv \frac{Z_C - Z_{C,O}}{Z_{C,F} - Z_{C,O}} = \frac{Z_C}{\mu_{C,CH_3OH}}, \quad \xi_H \equiv \frac{Z_H - Z_{H,O}}{Z_{H,F} - Z_{H,O}} = \frac{Z_H}{\mu_{H,CH_3OH}}.$$

A different formulation of the differential diffusion parameters is to compute correlations between ξ_C and ξ_H.

It is important to note that there is a fundamental limitation in the interpretation of the difference between ξ_C and ξ_H in terms of differential diffusion effects alone. The contribution to these quantities comes from carbon-carrying and hydrogen-carrying species in which the particular C and H may not play a significant role in its transport properties.

3.3 Flame propagation

The propagation of the flame may be tracked by evaluating a displacement speed of the front relative to the flow field. This quantity may be evaluated exactly from the numerical results when a flame surface is tracked with a particular scalar isocontour (such as hydrogen molecule mass fraction). An expression for the displacement speed, S_d, based on tracking a constant mass fraction contour may be obtained (Ruetsch *et al.*, 1995) by writing the Hamilton-Jacobi equation and substitution of the governing species equation:

$$\rho S_d \equiv \rho_u S_d^* = \frac{1}{|\nabla Y_\alpha|} \left[\frac{\partial}{\partial x_j} \left(\rho D_\alpha \frac{\partial Y_\alpha}{\partial x_j} \right) + \dot{\omega}_\alpha \right]. \tag{3}$$

In this expression, S_d^* is the density-weighted displacement speed. In this general form, the displacement speed measures the velocity of a scalar iso-contour (i.e. the flame-front) relative to the local gas. The value of S_d depends on the location in the flame where it is measured. The use of the product ρS_d or S_d^* tends to reduce thermal expansion effects due to the choice of the location where S_d is measured. Under strictly one-dimensional planar flame condition, this quantity is constant. In the reaction zone, the value of the density-weighted displacement speed, S_d^*, reflects primarily the chemical contribution. However, with the exception of perhaps a narrow region in the reaction zone, ρS_d is subject to additional effects resulting from the processes in the preheat zone.

A measure of the triple flame stabilization mechanisms is its speed relative to the cold gas. It may be evaluated using the same approach adopted by Ruetsch & Broadwell (1995). This speed contains both the contributions from chemical and hydrodynamic-diffusive effects (Echekki, 1992 & 1996; Poinsot *et al.*, 1992). To evaluate the hydrodynamic-diffusion contribution, the velocity, V_f, of the triple point relative to the unburnt gas is evaluated. V_f, at the leading edge of the flame, may be evaluated using the following relation:

$$V_f = (S_d - u_f) + u_0, \tag{4}$$

where u_f is the gas velocity at the flame location where the displacement speed is computed. The term $-S_d + u_f$ represents the Lagrangian speed of the triple point. The speed u_0 is the unburnt gas velocity at the inlet of the computational domain prior to the onset of lateral flow expansion and cross-stream diffusion effects. Note that, although S_d and u_f vary along the flame, the combined speed, $-S_d + u_f$, is constant in the flame under steady flow conditions.

4. General structure of the triple flame

In what follows, a description of the general structure of the methanol (CH_3OH)-air triple flame is given in terms of reactant, radicals, and heat release rate profiles.

4.1. Reactants and products profiles

Figure 2 shows the isocontours of the major species (reactants and products) mass fractions in the triple flame. The figure shows no leakage of the fuel beyond the primary premixed flame (Fig. 2c). Beyond the premixed flame front, methanol (CH_3OH) is decomposed into more stable fuels which include CO, H_2, and H. On the lean side, O_2 survives through the premixed flame and diffuses towards the stable reactants from the fuel side. A reduction in the fuel concentration across the premixed flame has also been observed by Terhoeven & Peters (1996) in their methane-air flame, albeit to a lesser extent. In addition to its oxidation by radical species in the C_1 chain, methanol pyrolyzes in the preheat zone (Seshadri *et al.*, 1989).

The reaction rates governing the premixed flame chemistry exhibit additional asymmetries, as shown in Fig. 3. The oxidation of methanol proceeds down the C_1 path: $CH_3OH \rightarrow CH_2OH \rightarrow CH_2O \rightarrow HCO \rightarrow CO \rightarrow CO_2$. The oxidation of methanol through HCO occurs in the premixed branches, whereas the remaining oxidation steps are present in all three branches. In addition to CO, the stable molecule H_2, which is produced on the rich premixed flame side, is also oxidized in the diffusion flame. All fuels in the premixed and diffusion flame are being oxidized primarily by radical species H, OH, and O. While H and OH play a more important role in the oxidation process on the rich premixed branch, oxidation reactions involving O atom play a more significant role on the lean side.

The reaction rates governing the premixed flame chemistry exhibit additional asymmetries, as shown in Fig. 3. For example, the peak production rates of H_2 and CO occur on the fuel rich side due to the consumption of H atom and OH by hydrocarbon intermediates. A further asymmetry appears in the inclination of the diffusion flame towards the lean premixed flame. This inclination may be primarily attributed to the rates of diffusion of H_2 relative to O_2 such that the reaction zone of the diffusion flame is at the stoichiometric mixture. The consumption rate of CO, as shown in Fig. 3e, also exhibits some inclination towards the lean branch. CO is consumed primarily by OH in the water gas shift reaction, an important reaction contributing to the overall heat release; the asymmetry is due to the peak production of OH occurring on the lean side due to the elementary chain branching reaction, $O_2 + H \rightleftharpoons OH + O$.

4.2. Radical profiles

Figure 4 shows the radical profiles for H, O, OH, and CH_2O in the flame. This figure shows that O and H atoms peak at the triple point. OH, on the other hand, peaks behind the primary reaction zones of the premixed flames and along

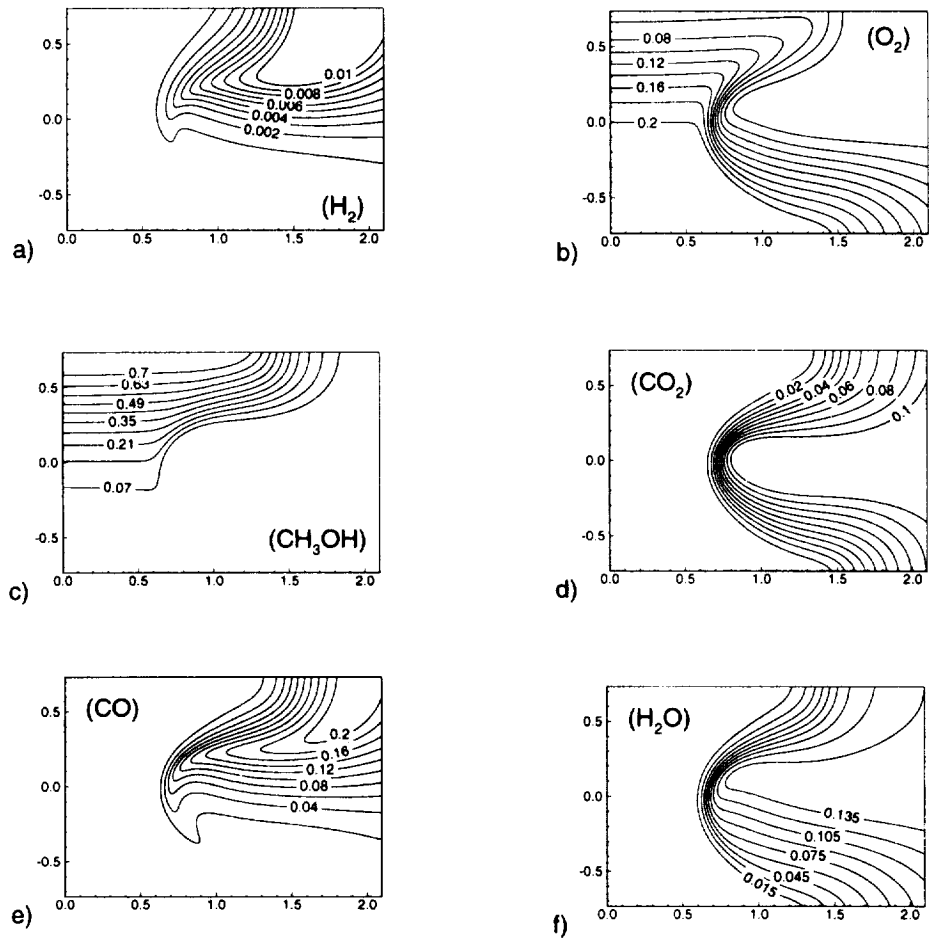

FIGURE 2. Major species mass fraction profiles (a) H_2, (b) O_2, (c) CH_3OH, (d) CO_2, (e) CO, and (f) H_2O.

the mean reaction zone of the diffusion flame branch. The radical OH has a slow recombination rate compared to O and H atoms and, therefore, accumulates and peaks in the diffusion flame.

Figure 5 shows the the contribution of the different reactions to the production and consumption of H, O, OH, and CH_2O. The radicals H, O, and OH are produced behind the fuel consumption layer near the burnt gas side of the flame, and diffuse upstream towards the unburnt gas to react in the fuel and radical consumption layer. The molecule H_2, on the other hand, is produced in the fuel and radical consumption layer and is consumed in the region of radical production in the H_2 oxidation layer. The convex shape of the triple point flame towards the burnt gas focuses H_2 towards its oxidation layer. The peak production of H_2 in the triple flame

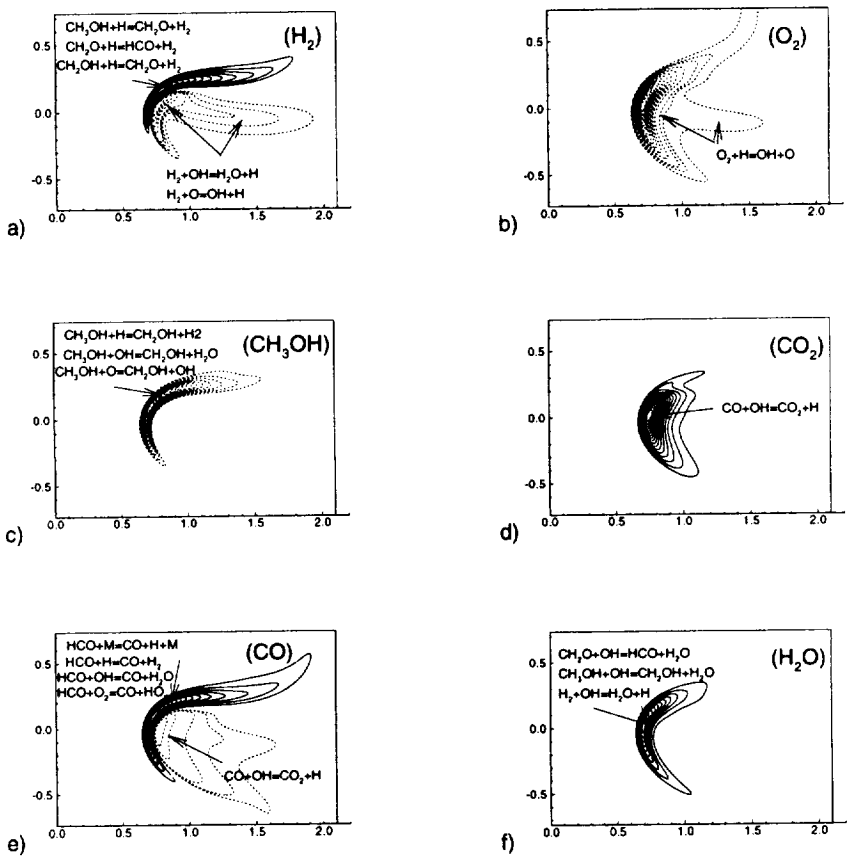

FIGURE 3. Major species reaction rate profiles (a) H_2, (b) O_2, (c) CH_3OH, (d) CO_2, (e) CO, and (f) H_2O. Production rates: ——— ; consumption rates: - - - - .

occurs at the triple point region on the rich side of the premixed flame. It results primarily from the break up of the fuel and its reactions with radicals, especially H. The primary mechanism for H_2 consumption results from radical production (in the H_2 oxidation layer) through the following reactions:

$$H_2 + OH \rightleftharpoons H_2O + H,$$

and

$$H_2 + O \rightleftharpoons OH + H.$$

The latter reaction is a significant chain branching reaction which plays a major role in the rate of flame propagation and radical production. By the focusing of H_2 towards its oxidation (consumption) zone, the rate of radical production is enhanced and the propagation speed is increased. An additional chain branching reaction which is responsible for the bulk of production of O and OH is the following reaction:

$$O_2 + H \rightleftharpoons O + OH.$$

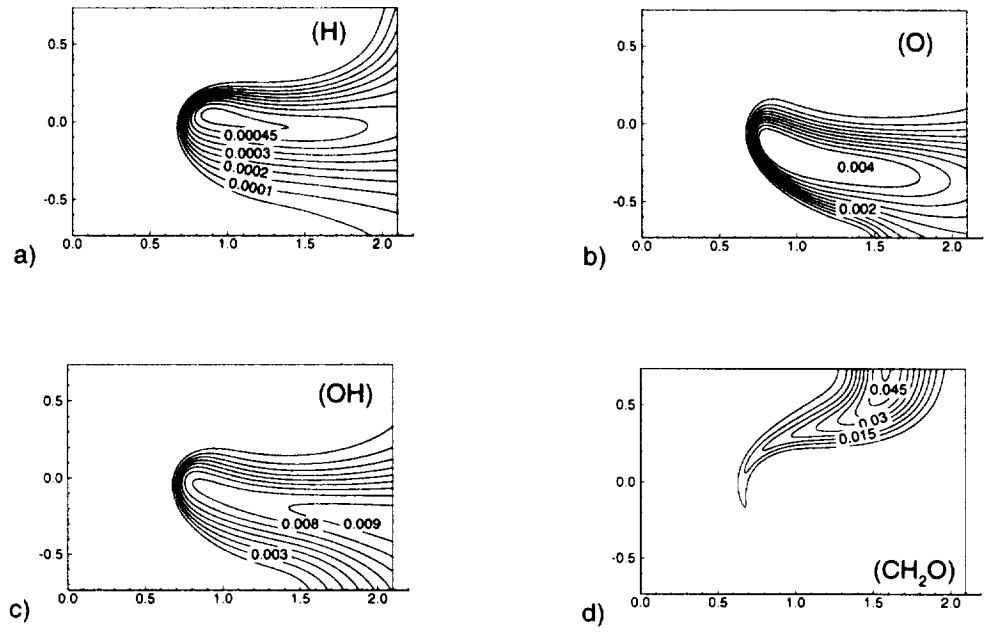

FIGURE 4. Minor species mass fraction profiles (a) H, (b) O, (c) OH, and (d) CH_2O.

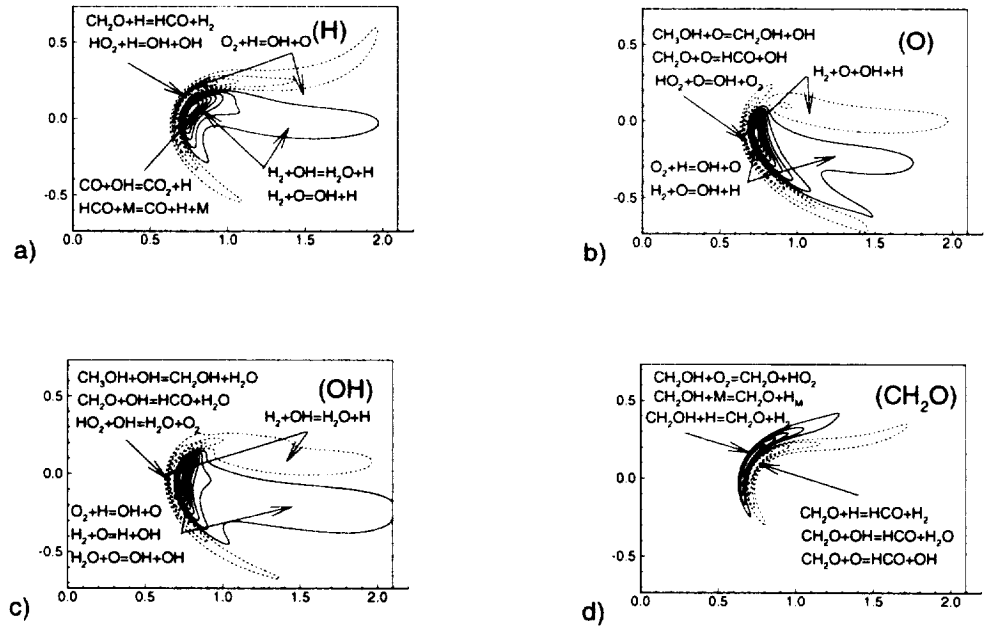

FIGURE 5. Minor species reaction rate profiles (a) H, (b) O, (c) OH, and (d) CH_2O. Symbols as in Fig. 3.

While the H atom in this reaction is defocused at the triple point by the same mechanism that focuses H_2, the net effect is the enhanced concentration of radical species at the triple point. The enhanced activity in this region also contributes to the ignition and anchoring of the trailing diffusion flame.

4.3. Parameterization of triple flame structure

The two-dimensional structure of the triple flame and the variation of the degree of premixedness in the reacting mixture suggest that at least two phase-space parameters may be required to fully describe the triple flame structure. Figure 6 shows overlays of the mixture fraction (Bilger *et al.*, 1990) profiles with H_2 reaction rate and temperature. The consumption rate of H_2 is used to illustrate the alignment of reaction rates in the diffusion flame with isocontours of the mixture fraction. The mixture fraction changes monotonically across the diffusion flame. This suggests that the mixture fraction may be a useful progress variable in this branch. Temperature plays a similar role in the premixed branches. In this section, we choose temperature and mixture fraction to parameterize the flame structure. The two parameters, ξ and T, effectively span the entire range of reaction and mixedness. The mixture fraction is a measure of the degree of mixedness, while the temperature is a measure of the extent of reaction.

Figures 7 and 8 show the mass fractions and reactions rates for the major species in phase space, while the corresponding figures for the minor species are shown in Figs. 9 and 10. Overlayed on these figures is the maximum consumption rate of O_2 in the premixed (thick solid lines) and the diffusion (thick dashed lines) branches. The maximum consumption rate of O_2, the only reactant which is consumed in the premixed and diffusion flames, is used to demarcate the three branches of the flame. These figures highlight the different topologies of the flame which may not be apparent in physical coordinates, particularly if the flame is distorted significantly by the flow field. Shifts in concentration or reaction peaks on the lean and rich sides and the delineation between diffusion and premixed branches are made more pronounced using this parameterization. Similarly the delineation of reactions and species that are present in the premixed branches versus the diffusion flame is made more clear. For example,

1. the peak production rates for formaldehyde (CH_2O), H_2 and CO occur on the rich side of the flame in the premixed branch, while the peak consumption of H_2 and CO persists to very lean conditions;

2. the peak consumption of H occurs on the rich side, whereas the peak consumption of O atoms occurs on the lean side of the flame;

3. the peak concentrations of CH_2O, H_2, and CO exist well into the rich side;

4. the peak radical concentrations for O and H exist near the triple point and on the lean sides respectively, whereas OH peaks in the diffusion flame;

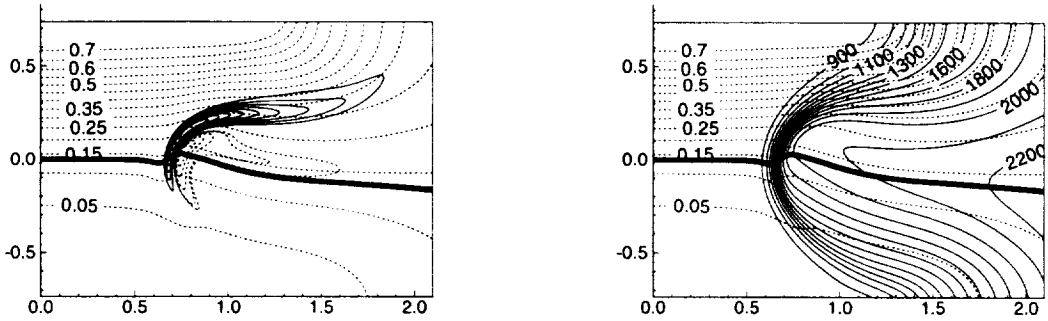

FIGURE 6. Overlay of mixture fraction profiles with H_2 reaction rate (left) and temperature (right). The wide solid line denotes the stoichiometric mixture fraction isocontour. The mixture fraction isocontours are shown in dashed lines.

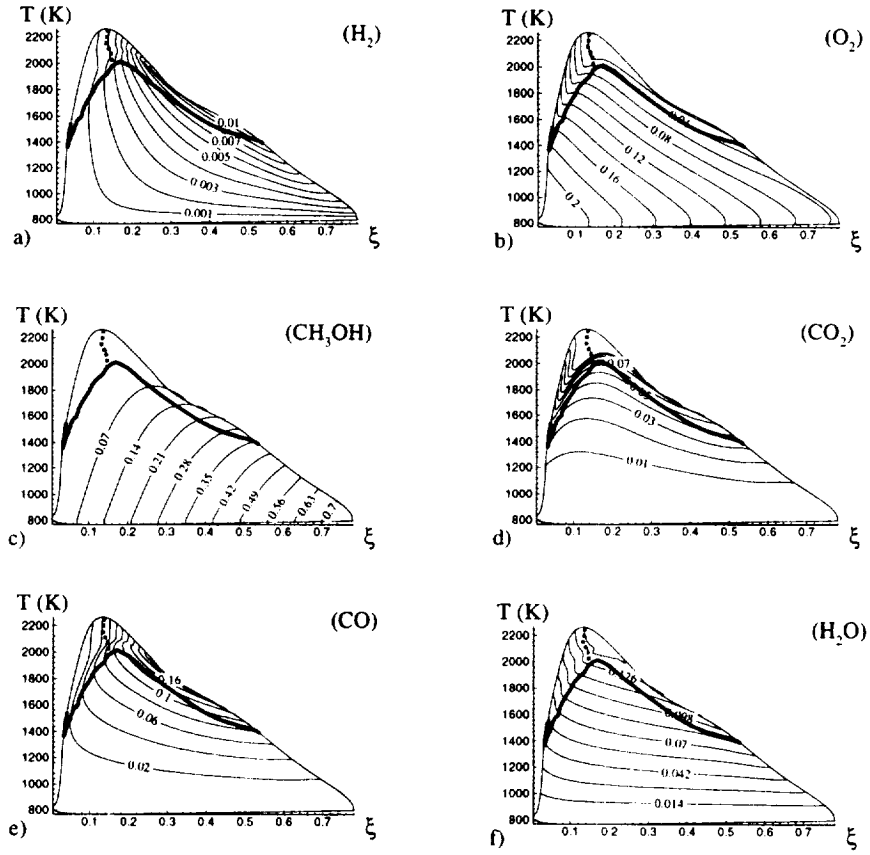

FIGURE 7. Major species mass fraction for H_2, O_2, CH_3OH, CO_2, CO and H_2O in ξ-T phase space. The bold solid line demarcates the premixed branches. The bold dashed line demarcates the diffusion branch.

5. while O_2 exists behind the premixed flame, there is no leakage of methanol or formaldehyde behind the premixed branches.

5. Propagation of the triple flame and its stabilization

In this section, the values of the propagation speeds are reported using the mass fraction of H_2 to track the flame surface. Other scalars yield similar results. The ratio of density-weighted displacement speed, S_d^*, to the laminar stoichiometric flame value, S_L, at the leading edge of the triple flame is 1.13. Since S_d^* is measured in the reaction zone, its enhancement relative to the laminar value is primarily attributed to an enhancement in the burning intensity of the flame (Sec. 3.3) due to the coupling of differential diffusion with curvature.

Another quantity of relevance to the stabilization mechanism of the triple flame is the flame speed relative to the unburnt gas, V_f (Sec. 3.3). The ratio, $V_f/S_{L,\phi=1}$, based on H_2 mass fraction is 1.79. The approximately 80% enhancement in V_f may be attributed primarily to hydrodynamic-diffusive effects associated with lateral flow expansion and cross-stream diffusion. Ruetsch *et al.* (1995) show that the ratio, $V_f/S_{L,\phi=1}$, may be approximated by the square-root of the inverse density ratio across the flame, $\sqrt{\rho_u/\rho_b}$, or by the temperature ratio, $\sqrt{T_b/T_u}$. In the current computation, the quantity $\sqrt{T_b/T_u} \sim \sqrt{2300/800} \sim 1.7$ compares well with the computational values for $V_f/S_{L,\phi=1}$ after subtraction of the chemical contribution.

6. Differential diffusion effects

In the previous sections, we have identified some contributions to the triple flame structure which result from differential diffusion effects: (a) the inclination of the diffusion branch towards the lean premixed branch, (b) the enhancement of the displacement speed, and (c) the ignition at the triple point. There are a number of approaches in the literature which attempt to quantify these effects. In this section, two approaches to investigate differential diffusion effects are compared. Figure 11 shows correlations of the elemental mixture fractions based on C and H in the triple flame. Elemental mixture fractions may only be modified by transport since reaction does not modify the atomic composition of a mixture. The figure shows that on the unburnt gas side, the values of ξ_C and ξ_H are the same, and that both reflect the local unburnt gas composition of the methanol (the correlation is shown by the diagonal line of ξ_C vs. ξ_H). In the reaction zone of the premixed branches, ξ_C is smaller than ξ_H, although this difference is not significant and it reflects the production of relatively fast diffusive species such as H_2. The difference between the two quantities is reversed behind the rich branch. There, the greatest contribution to ξ_C comes from CO, while the main contribution to ξ_H is from H_2O and H_2. In this region, the deficit in H may be a result of the diffusion of H_2 and H towards the diffusion flame. On the oxidizer side of the diffusion flame, ξ_C is lower than ξ_H. In this region, the main contribution to ξ_H is from H_2O, and for ξ_C is CO_2. There is no distinct behavior at the triple point from ξ_C and ξ_H contours. The

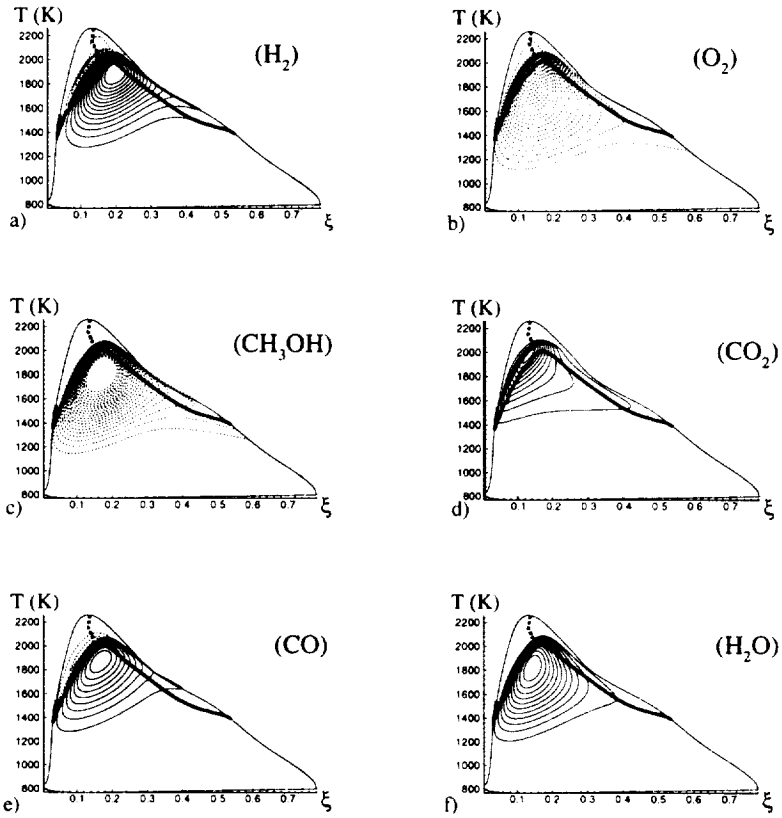

FIGURE 8. Major species reaction rate for H_2, O_2, CH_3OH, CO_2, CO and H_2O in ξ-T phase space. Symbols as in Fig. 7.

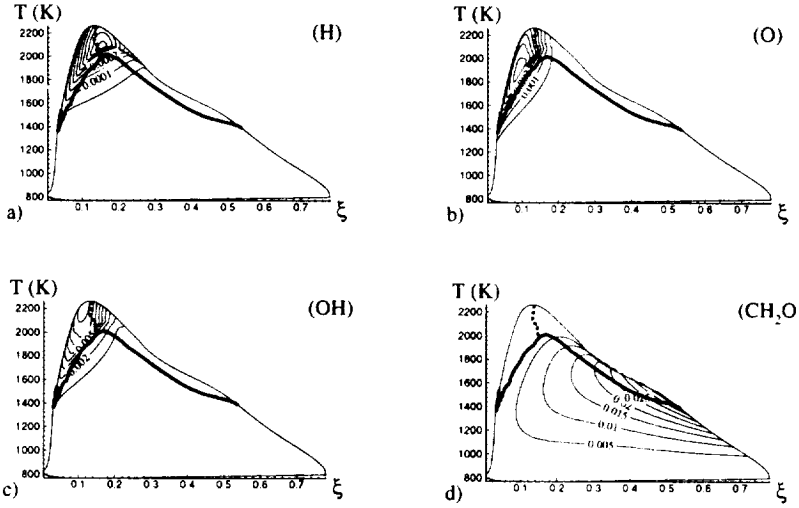

FIGURE 9. Minor species mass fraction for H, O, OH and CH_2O in ξ-T phase space. Symbols as in Fig. 7.

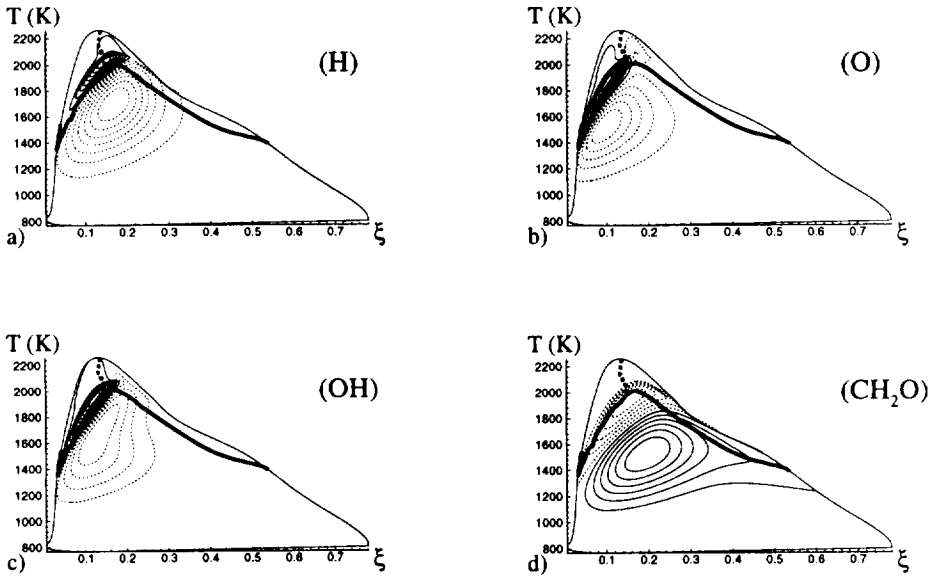

FIGURE 10. Minor species reaction rate for H, O, OH, and CH_2O in ξ-T phase space. Symbols as in Fig. 7.

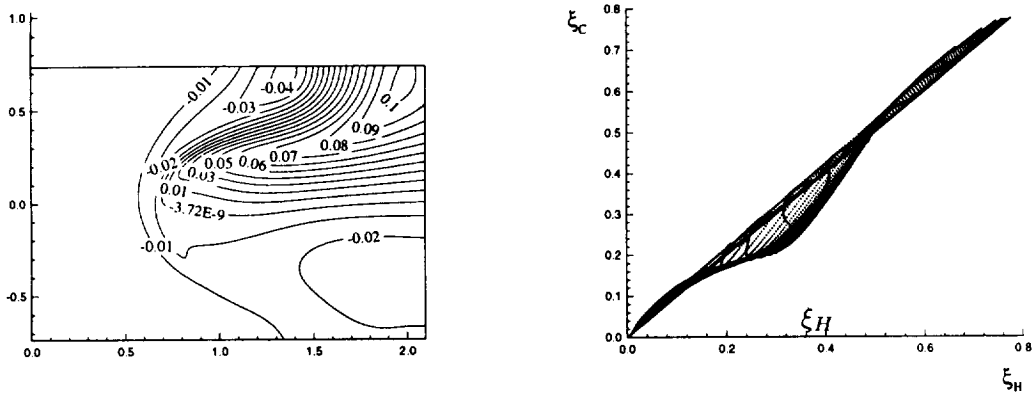

FIGURE 11. Correlation of C and H elemental mixture fractions. Left: $\xi_C - \xi_H$; right: ξ_C vs. ξ_H.

principal limitation of the mixture fraction approach as a measure of differential diffusion effects is now more apparent; the value of the elemental mixture fraction does not tell us whether the higher or lower element composition in a given region is a result of its transport by a species which is fast or slow diffusing. Hydrogen, for example, may be present in both H_2O or H_2, but the two species have very different diffusivities. At the triple point, minor species such as H atom may not contribute

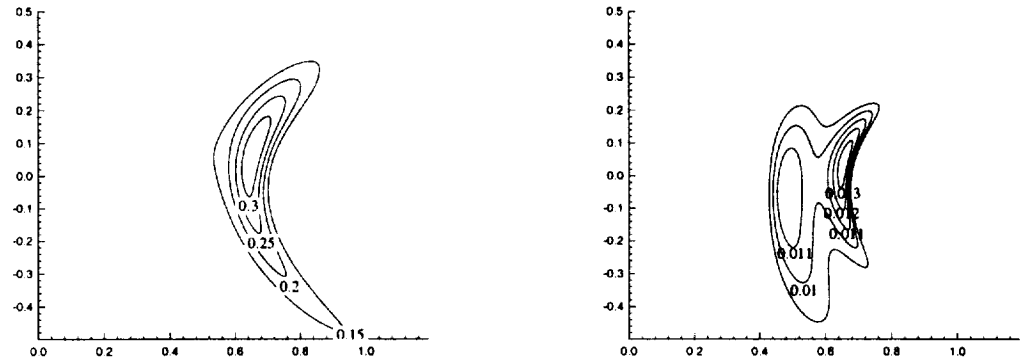

FIGURE 12. Diffusion velocities of H and CO normalized by the stoichiometric one-dimensional flame speed. Left: V_H/S_L; right: V_{CO}/S_L.

significantly to the elemental mixture fraction despite their important role in the chemistry of the flame.

Another indication of the role played by diffusional transport and its coupling with curvature may be demonstrated by the magnitudes of the diffusion velocity of H and CO shown in Fig. 12. This figure shows that the maximum diffusion velocity is found near the triple point of the flame. This velocity corresponds to more than a two-fold increase for H relative to the remaining premixed branches. The increase in the diffusion velocity of CO is only 30%. The peak value of the diffusive velocity for H is approximately thirty times higher than that of CO. The use of diffusion velocities to quantify differential diffusion effects shows significantly different trends than the elemental mixture fraction approach.

7. Concluding remarks

The structure, propagation and stabilization mechanisms of a methanol-air triple flame is investigated using DNS. The computations show that the primary fuel, methanol, is consumed entirely through the premixed branches of the flame and is converted to more stable fuels, H_2 and CO, for the diffusion flame behind the triple point.

In the triple point region, the coupling of curvature and differential diffusion of hydrogen molecules results in enhanced radical production and, in turn, an enhancement in the flame propagation speed. However, hydrodynamic effects (associated with heat release in the flame) are more important in the current computations. These effects are predicted adequately by the model by Ruetsch *et al.* (1995).

A mixture fraction-temperature parameterization of the triple flame structure is proposed. The approach attempts to separate mixedness and reactivity, and highlights some of the interesting features of partially-premixed combustion.

A comparison between two approaches to identify the effects of differential diffusion is carried out. The first approach is based on a direct computation of the magnitude of the diffusion velocity of the various species. The second is based on the comparison of elemental mixture fractions based on carbon and hydrogen atoms. The comparison between the two approaches shows that the second approach is strongly dependent on the species carrying the atoms and may not be a good indicator of differential diffusion effects.

Acknowledgments

This research was supported by the United States Department of Energy, Office of Basic Energy Sciences, Chemical Sciences Division. We would like to thank Profs. Amable Liñán and Forman Williams, and Drs. Greg Reutsch and Arnaud Trouvé for many fruitful discussions.

REFERENCES

BILGER, R. W. 1981 Molecular Transport effects in turbulent diffusion flames at moderate Reynolds number. *AIAA J.* **20**(7), 962-970.

BILGER, R. W. & DIBBLE, R. W. 1982 Differential molecular diffusion effects in turbulent mixing. *Combust. Sci. & Tech.* **28**, 161-172.

BILGER, R. W., STARNER, S. H. & KEE, R. J. 1990 On Reduced Mechanisms for Methane-Air Combustion. *Combust.& Flame.* **80**, 135-149.

CARD, J. M., CHEN, J. H., DAY, M. & MAHALINGAM, S. 1994 Direct Numerical simulations of turbulent non-premixed methane-air flames modeled with reduced kinetics. *Proceedings of the 1994 Summer Program,*Center for Turbulence Research, NASA-Ames/Stanford University, 41-54.

DOMINGO, P. & VERVISCH, L. 1996 Triple Flames and partially premixed combustion in autoignition of nonpremixed turbulent mixtures. To appear in *Twenty-Sixth Symposium (International) on Combustion*, The Combustion Institute, Pittsburgh.

DRAKE, M. C. & BLINT, R. J. 1988 Structure of laminar opposed-flow diffusion flames with $CO/H_2/N_2$ Fuel. *Combust. Sci. & Tech.* **61**, 187-224.

ECHEKKI, T. 1992 Studies of curvature, strain and unsteady effects on laminar premixed flames. Ph.D. Thesis, Mechanical Engineering Dept., Stanford University.

ECHEKKI, T. 1996 A quasi-one dimensional premixed flame model with cross-stream diffusion. To appear in *Combust. & Flame.*

HARTLEY, L. J. & DOLD, J. W. 1991 Flame propagation in a nonuniform mixture: analysis of a propagating triple-flame. *Combust. Sci. & Tech.* **80**, 23-46.

KENNEDY, C. J. & CARPENTER, M. H. 1994 Several new numerical methods for compressible shear-layer simulations. *Appl. Num. Math.* **14**, 397-443.

KENNEDY, C. J. & CARPENTER, M. H. 1996 Several New ultra-low-storage, lower-order Runge-Kutta schemes. In preparation.

KIONI, P. N., ROGG, B., BRAY, N. C. & LIÑÁN, A. 1993 Flame spread in laminar mixing layers: the triple flame. *Combust. & Flame.* **95,** 276-290.

LAKKARAJU, N. K. 1996 Studies of quenched diffusion flames near cold, inert surfaces. *Master's Thesis,* Dept. of Mechanical Engineering, Michigan State University, Lansing, MI.

MASRI, A. R., DIBBLE, R. W. & BARLOW, R. S. 1992 The structure of turbulent nonpremixed flames of methanol over a range of mixing rates. *Combust. & Flame.* **89,** 167-185.

POINSOT, T., ECHEKKI, T. & MUNGAL, M. G. 1992 A study of the laminar flame tip and implications for premixed turbulent combustion. *Combust. Sci. & Tech.* **81,** 45-73.

POINSOT, T. & LELE, S. 1991 Boundary Conditions for direct simulations of compressible viscous flows. *J. Comput. Phys.* **101,** 104-129.

RUETSCH, G. R. & BROADWELL, J. E. 1995 Effects of confinement on partially premixed flames. *Annual Research Briefs 1991.* Center for Turbulence Research, NASA-Ames/Stanford Univ.

RUETSCH, G. R., VERVISCH, L. & LIÑÁN, A. 1995 Effects of heat release on triple flames. *Phys. Fluids.* **7**(6), 1447-1454.

SESHADRI, K., TREVINO, C. & SMOOKE, M. D. 1989 Analysis of the structure and mechanisms of extinction of a counterflow methanol-air diffusion flame. *Combust. & Flame.* **76,** 111-132.

SMITH, L. L., DIBBLE, R. W., TALBOT, L., BARLOW, R. S. & CARTER, C. D. 1995 Laser Raman scattering measurements of differential molecular diffusion in turbulent nonpremixed jet flames of H_2/CO_2 Fuel. *Combust. & Flame.* **100,** 153-160.

SMOOKE, M. D. & GIOVANGIGLI, V. 1991 *Reduced kinetic mechanisms and asymptotic approximation for methane-air flames* (M. D. Smooke, Ed.), Lecture Notes in Physics 384, Springer-Verlag, New York, 1-28.

TERHOEVEN, P. & PETERS, N. 1996 Basic flame structures of turbulent combustion for applications in diesel engines. To appear in *Combust. & Flame.*

WARNATZ, J., MAAS, U. & DIBBLE, R. W. 1996 *Combustion: physical and chemical fundamentals, modeling and simulation, experiments, pollutant formation.* Springer-Verlag, Berlin Heidelberg, Germany.

WICHMAN, I. S. 1995 Basic features of triple flames in combustion theory. To appear in Eighth International Symposium on Transport Processes in Combustion (ISTP-8), San Francisco.